



OPEN Apical-out intestinal organoids as an alternative model for evaluating deoxynivalenol toxicity and *Lactobacillus* detoxification in bovine

Min Gook Lee¹, Bo Ram Lee¹, Poongyeon Lee¹, Soyoung Choi², Jong-Hui Kim³, Mi-Hwa Oh³ & Jae Gyu Yoo¹✉

Small intestinal organoids are similar to actual small intestines in structure and function and can be used in various fields, such as nutrition, disease, and toxicity research. However, the basal-out type is difficult to homogenize because of the diversity of cell sizes and types, and the Matrigel-based culture conditions. Contrastingly, the apical-out form of small intestinal organoids is relatively uniform and easy to manipulate without Matrigel. Therefore, we sought to investigate the possibility of replacing animal testing with bovine apical-out small intestinal organoids (Apo-IOs) by confirming the toxicity of mycotoxins and effectiveness of *L. plantarum* as mycotoxin-reducing agents. The characteristics and functions of Apo-IOs were first confirmed. The gene and protein expression of stem cell, proliferation, mucous, and adherence markers were detected, and the absorption capacity of amino and fatty acids was also confirmed. FITC-4 kDa dextran, a marker of intestinal barrier function, did not penetrate the Apo-IOs, confirming the role of the organoids as a barrier. However, when co-treated with deoxynivalenol (DON), FITC-4 kDa dextran was detected deep within the organoids. Moreover, qPCR and immunofluorescence staining confirmed a decrease in the expression of key markers, such as LGR5, Ki67, Mucin2, Villin2, and E-cadherin. In addition, when Apo-IOs were treated with *Lactobacillus plantarum* ATCC14917 culture supernatant (LCS) and DON together, cell death was reduced compared to when treated with DON alone, and FITC-4 kDa dextran was confirmed to flow only to the peripheral part of the organoid. The qPCR and immunofluorescence staining results of LCS and DON co-treatment group showed that LGR5, Ki67, Mucin2, Villin2, and E-cadherin were expressed at significant higher levels than those in the DON treatment group alone. In this study, we found that the characteristics and functions of bovine Apo-IOs were similar to those of the intestinal structure in vivo. Additionally, the effects of mycotoxins and effectiveness of *L. plantarum* as mycotoxin-reducing agents were confirmed using bovine Apo-IOs. Therefore, bovine Apo-IOs could be applied in toxicity studies of mycotoxins and could also be used as in vitro models to replace animal testing and improve animal welfare.

Keywords Deoxynivalenol, Mycotoxin, Intestinal organoid, Bovine

Abbreviations

Apo-IOs	Apical-out small intestinal organoids
Bo-IOs	Basal-out small intestinal organoids
DAPI	4',6-diamidino-2-phenylindole
DON	Deoxynivalenol
ISC	Intestinal stem cell

¹Animal Biotechnology Division, National Institute of Animal Science, Rural Development Administration, Wanju, Republic of Korea. ²Animal Genomics and Bioinformatics Division, National Institute of Animal Science, Rural Development Administration, Wanju, Republic of Korea. ³Animal Products Research and Development Division, National Institute of Animal Science, Rural Development Administration, Wanju, Republic of Korea. ✉email: vetjack@korea.kr

LCS	<i>Lactobacillus plantarum</i> ATCC14917 culture supernatant
PI	Propidium iodide
PBS	Phosphate-buffered saline
FITC	Fluorescein isothiocyanate
LGR5	Leucine-rich repeat containing G protein-coupled receptor 5
ANOVA	Analysis of variance
BODIPY	Fluorescence-labeled fatty

Organoids are three-dimensional (3D) structures derived from stem cells, characterized by their capacity for self-renewal, self-organization, and differentiation into diverse cell types that accurately mimic the functions and structure of their tissue of origin *in vivo*^{1,2}. Small intestinal organoids were first developed in mice, and three-dimensional intestinal organoids can imitate intestinal epithelial cells *in vivo*³. It has since been developed in humans, farm animals, and companion animals^{4,5}. The development of small intestinal organoids addressed the limitations of existing 2D-based *in vitro* cell models, which are constrained by the presence of only one cell type and the absence of the complex structure inherent in intestinal tissue. The developed small intestinal organoids have been used in various studies, including host-microbial interaction⁶, infectious^{7–10}, and toxicity studies¹¹.

Generally, the small intestine acts as a physical and immunological barrier against harmful elements, such as detrimental microbes and toxins, as well as for the digestion and absorption of nutrients¹². Small intestinal organoids possess a crypt-villus structure akin to that of the actual small intestine and can differentiate into various cell types originating from intestinal stem cells. Small intestinal organoids are used in various fields of human research. For example, small-molecular substances, known to cause diarrhea in humans, can be treated with small intestinal organoids to produce changes in the intestinal epithelium, similar to that for clinically observed diarrhea, which can be used to study the mechanism of diarrhea and various drugs. Moreover, they have proven useful in developmental studies and safety evaluations¹³. Intestinal organoids were used to investigate immune and inflammatory responses after coinoculation of viruses in pigs⁹. They have also been used to study the toxicity of mycotoxins in pigs¹¹. By treating pig intestinal organoids with deoxynivalenol (DON), it was confirmed that the mycotoxin not only inhibited the Wnt/ β -catenin pathway, which is essential for the self-renewal and differentiation of intestinal epithelial cells, but also reduced the protein levels of β -catenin and Lgr5¹¹. However, they have structural drawbacks, as the basal surface is exposed externally, unlike the *in vivo* small intestine, where the apical side faces the lumen. Therefore, their use in experiments on nutrient absorption, toxicity assessments, and microbial treatments is limited. Recently, chicken apical-out intestinal organoids (Apo-IOs) were used in a toxicity study with mycotoxins to confirm intestinal barrier damage and the weakened expression of related proteins¹⁴.

Mycotoxins, including aflatoxins, ochratoxin, zearalenone, and DON, are secondary metabolites produced by fungi. DON is commonly found worldwide in grains, such as wheat, barley, and corn^{15,16}. In livestock, such as pigs and chickens, ingestion of DON-contaminated feed impairs nutrient absorption, compromises the intestinal barrier function, and weakens immune responses¹⁷. Consequently, economic losses occur due to a decrease in livestock feed intake, growth, and reproductive functions^{18,19}. In the livestock industry, the intake of DON-contaminated grains can lead to reduced milk production in dairy cows and weight loss in pigs, as well as symptoms such as food refusal, vomiting, and diarrhea, ultimately leading to economic losses²⁰. DON, which is absorbed in the small intestine, negatively affects nutrient absorption, immunity, and barrier integrity. Barrier integrity of the small intestine is maintained by tight junction proteins, adherent junctions, desmosomes, and gap junctions²¹. DON inhibits protein synthesis and increases permeability of the intestinal monolayer and barrier^{22,23}. The compromised integrity leads to an increase in permeability and damages intestinal barrier function²⁴.

To mitigate the toxicity of DON, various methods, including physical, chemical, and lactic acid bacteria treatments are used to reduce the toxicity of DON. Physical methods include degradation, irradiation, light treatment, ultrasound treatment, ozone, and atmospheric cold plasma treatment, whereas chemical methods include alkaline, chlorine, ammonium carbonate, sodium bisulfite, sodium metabisulfite, sodium carbonate, L-ascorbic acid, and L-cysteine treatments²⁵. Probiotic metabolites have been confirmed to be effective at inhibiting the growth of *Fusarium* spp. by producing various bacterial metabolites²⁶. Probiotics are live organisms present in food that produce beneficial effects, such as maintaining the intestinal environment, regulating the immune system, and producing metabolites necessary for intestinal health²⁷. Among these, *Lactobacillus* is the most commonly used probiotic. Previous studies have confirmed that the addition of *Lactobacillus* to a porcine jejunal explant model reduces enteritis and oxidative stress caused by DON^{17,28,29}. In a previous study, we constructed a basal-out intestinal organoid (Bo-IOs) in cattle³⁰. In this study, we aimed to induce Bo-IOs into Apo-IOs and investigate their characteristics and functions. By evaluating the toxicity of mycotoxins using Apo-IOs and confirming the effectiveness of mycotoxin-reducing agents, we explored their potential as alternative *in vitro* models for toxicity assessments.

Results

Characterization of bovine apical-out intestinal organoids

Using the previously reported Bo-IOs (28), we induced Apo-IOs and characterized their configuration by examining their gene and protein expression. Specifically, we assessed expression of the small intestine markers of stem cells (LGR5), proliferation (Ki67), mucous production (Mucin2), villus formation (Villin2), and cell adhesion (E-cadherin). Unlike the budding-shaped Bo-IOs, polarity reversal was observed in the Apo-IOs (Fig. 1a, b). Using scanning electron microscopy (SEM) to observe Apo-IOs, it was found that the surface of Apo-IOs is covered with microvilli (Fig. 1c). We conducted quantitative real-time PCR to investigate the mRNA expression of genes with various functions to determine the characteristics of the two types of organoids. The

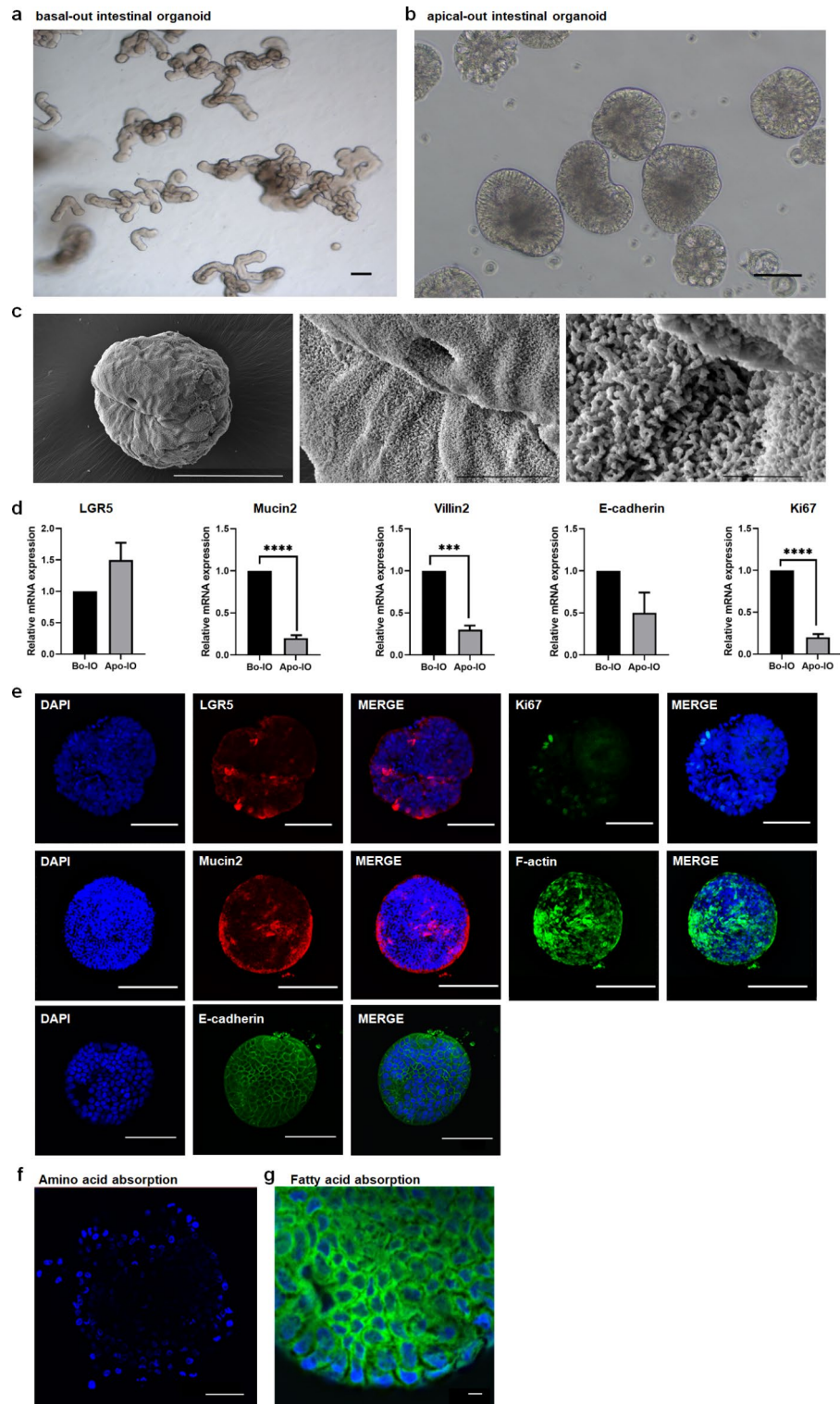


Fig. 1. Characterization of bovine apical-out intestinal organoids **a** Bovine basal-out intestinal organoids at passage 16 Scale bar = 200 μm . **b** Bovine apical-out intestinal organoids. Scale bar = 100 μm . **c** Representative scanning electron microscopy images of Ap-IOs. The surface of Ap-IOs is covered with microvilli. Scale bar = 50 μm (left), 10 μm (center), 2 μm (right). **d** Gene expression of stem cell (LGR5), proliferation (Ki67), mucous production (Mucin2), villus formation (Villin2), and cell adherence junction (E-cadherin) markers were compared between basal-out and apical-out organoids using qPCR. **e** Protein expression of LGR5, Ki67, F-actin, Mucin2, and E-cadherin was confirmed in the apical-out organoids using immunostaining. Nuclei were stained with 4',6-diamidino-2-phenylindole (DAPI; blue). Scale bar = 10 μm (a), 100 μm (b, c). **f** Amino acid absorption (blue) of the bovine apical-out intestinal organoid. Scale bar = 10 μm . **g** Fatty acid absorption (green) of the bovine apical-out intestinal organoids. The nuclei were stained with DAPI (blue). Scale bar = 10 μm .

results showed that the expression of Ki67, Mucin2, and Villin2 was significantly higher in Bo-IOs than in Apo-IOs ($P < 0.05$). No significant difference was observed in the expression of LGR5 and E-cadherin (Fig. 1d). At the protein expression level, small intestine-specific protein expression was normal in Apo-IOs. As shown in Fig. 1e, the immunofluorescence staining results showed that LGR5 and Ki67 were specifically expressed on the cell surface and in the nucleus, respectively. In addition, specific expression of Mucin2 secreted by goblet cells, as well as adherent junction (E-cadherin) and cytoskeleton (F-actin) proteins, were observed (Fig. 1e).

To investigate the ability of Apo-IOs to absorb nutrients, which is one of the functions of the small intestine, we examined the absorption capacity of amino and fatty acids. We used an amino acid analog with a fluorescent substance to confirm amino acid absorption ability. As a result, the nuclear region of the Apo-IOs exhibited a blue fluorescence, indicating amino acid absorption (Fig. 1f), while fatty acid absorption was indicated by green fluorescence in the perinuclear (Fig. 1g).

Application of bovine apical-out intestinal organoids in assessing the toxic effects of deoxynivalenol

PI (propidium iodide) identifies dead cells based on the principle that it penetrates and stains their damaged membranes. As the exposure time of Apo-IOs to DON increased, more PI staining was observed (Fig. 2a). Based on time-course cell viability assessments revealed a decline in cell viability to approximately 48% after 6 h of DON exposure, which further decreased to 17% after 8 h (Fig. 2b). To check whether the barrier of the Apo-IOs was intact, we confirmed that FITC-4 kDa dextran did not permeate into them. After 6 h of DON treatment, FITC-4 kDa dextran penetrated the Apo-IOs and accumulated in their central region (Fig. 2c). When comparing gene expression between the DON-untreated control and DON-treated groups, the gene expression of LGR5 and Ki67 decreased by approximately fivefold, that of Mucin2 decreased by approximately sixfold, and that of E-cadherin decreased by approximately 45-fold (Fig. 2d). The protein expression levels of LGR5 and E-cadherin decreased significantly in the DON-treated group. The expression of Ki67, Mucin2, and F-actin was absent in the nucleus and cytoplasmic membrane (Fig. 2e).

Effect of *Lactobacillus plantarum* ATCC14917 culture supernatant on deoxynivalenol with intestinal apical-out organoids

In this study, approximately 99.8% of the cells treated with the coincubation of LCS with Apo-IOs were found to be alive, and no significant difference was observed compared to Apo-IOs with no LCS. These results showed that LCS did not affect the survival rate of Apo-IOs. Subsequently, compared with the control group (DON only), co-treatment with DON + LCS significantly reduced the survival rate. However, the survival rate of apical-out intestinal organoids was significantly increased from 48 to 82.75% compared with that of DON alone (Fig. 3a). Unlike the control group, when FITC-4 kDa dextran was treated with LCS co-incubated Apo-IOs, it could not penetrate into the Apo-IOs. These results confirmed that LCS may help maintain the intestinal barrier of the intestinal barrier. Furthermore, only limited diffusion of FITC-4 kDa dextran into Apo-IOs was observed in the LCS-treated group, suggesting that *L. plantarum* alleviates DON-induced barrier dysfunction. These results also suggest that LCS enhances some of the barrier functions (Fig. 3b). Comparing the gene expression of the control and LCS, the gene expression of LGR5 and Ki67 increased by approximately fourfold, that of Mucin2 increased by approximately sixfold, and that of E-cadherin increased by approximately 7.5-fold. However, no significant difference in the expression of Villin2 was observed (Fig. 3c). Comparison of gene expression between the DON and DON + LCS revealed that gene expression in the DON + LCS group was approximately 1.5-fold higher for LGR5 and approximately two-fold higher for Mucin2 and Ki67, whereas E-cadherin in the DON-treated group increased by approximately 23-fold. In addition, the gene expression of Villin2, which was not expressed in the DON-treated group, was expressed in the DON + LCS group (Fig. 3d). Protein expression analysis in the DON + LCS group showed strong expression of LGR5, while Ki67, F-actin, and E-cadherin were partially expressed. Moreover, Mucin2 expression was not observed (Fig. 3e).

Discussion

The small intestine is composed of enterocytes and goblet, Paneth, and enteroendocrine cells. Using small intestinal organoids in an apical-out orientation, which more accurately mimics the natural orientation of intestinal cells in vivo, is often preferable to using Bo-IOs. If basal-out organoids are used, various methods have to be included, such as (i) microinjection to deliver experimental agents into the center of the spheroid^{31,32} and (ii) dissociation of 3D organoids and re-seeding cells onto cell culture inserts to generate 2D monolayers³³. However, the microinjection method has the disadvantage of requiring expertise, engineering knowledge, and specialized equipment, while the induction of 2D monolayers requires a large number of cells and an extended period for cell maturation and differentiation. Furthermore, there are two advantages when Apo-IOs are applied: (i) Apo-IOs have uniform sizes, whereas basal-out organoids have different sizes; (ii) Since Apo-IOs are cultured in suspension without Matrigel, they allow for uniform exposure to drugs or toxins, making them particularly suitable for studies on drug effects or toxicity³⁴.

The shape of Apo-IOs was observed using an optical microscope and SEM. The results showed that Apo-IOs had a round shape, unlike Bo-IOs, with an average size of 100 to 150 μm . Additionally, SEM imaging revealed that the surface of Apo-IOs was covered with microvilli, which were similarly exposed on the outer surface like human Apo-IOs generated from human embryonic stem cells³⁵. These findings suggest that the Apo-IOs, with their uniform size and exposed microvilli, could be applied in various research fields, addressing some limitations of conventional small intestine organoids. LGR5 is expressed within the crypt of the small intestine and induces the differentiation of small intestine epithelial cells; Ki67 induces cell proliferation in the small intestine; E-cadherin plays the role of adherens junctions; Mucin2 forms the small intestinal mucosa; and Villin2 plays a role in small intestine villi formation^{3,36}. We identified and confirmed the gene and protein expression

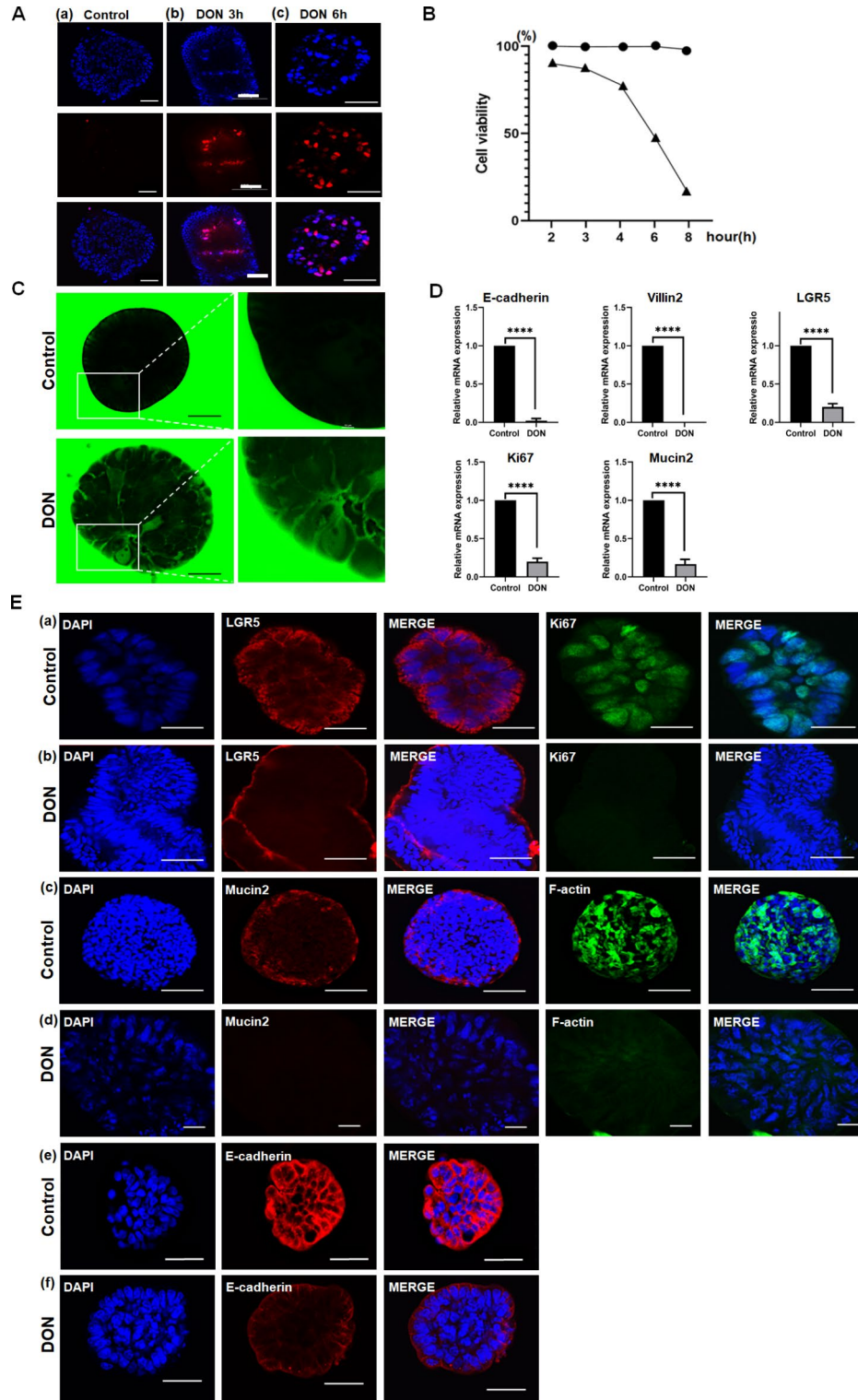


Fig. 2. Toxic effect of deoxynivalenol (DON) on bovine apical-out intestinal organoids. **a** To determine the LC50 value, bovine apical-out intestinal organoids were treated with 25 μ M DON and stained with propidium iodide (PI) for each time period. Nuclei were stained with 4',6-diamidino-2-phenylindole (DAPI; blue). Scale bar = 50 μ m (a), 100 μ m (b, c). **b** Results indicated for 25 μ M DON treatment for 6 h. **c** Permeability of apical-out intestinal organoids induced by DON. Scale bar = 10 μ m. **d** Effect of 25 μ M DON treatment on the gene expression of apical-out intestinal organoids. **e** Effect of 25 μ M DON treatment on the protein expression of apical-out intestinal organoids. Nuclei were stained with DAPI (blue). Scale bar = 100 μ m (a-c, e, f). 10 μ m (d).

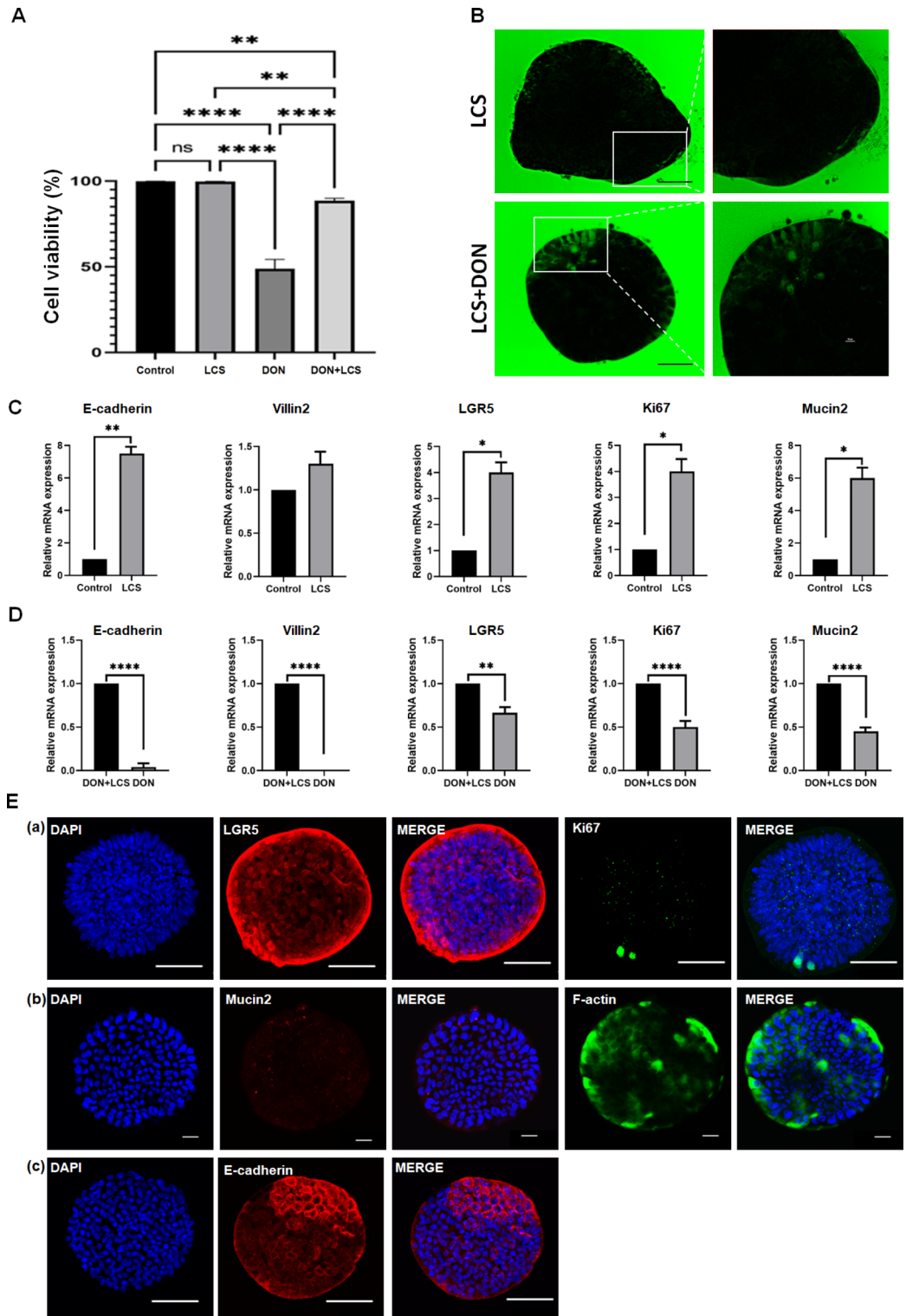


Fig. 3. Alleviated effect of *Lactobacillus plantarum* ATCC14917 culture supernatant (LCS) on bovine apical-out intestinal organoids. **a** Comparison of the cell viability in the control, LCS, deoxynivalenol (DON), and DON + LCS treatment groups. **b** Permeability of apical-out intestinal organoids induced by LCS and DON + LCS treatment. Scale bar = 50 μ m. **c** Effect of LCS on the gene expression of apical-out intestinal organoids. **d** Comparison of gene expression between DON and DON + LCS treatments. **e** Effect of DON + LCS treatment on the protein expression of apical-out intestinal organoids. Nuclei were stained with 4',6-diamidino-2-phenylindole (DAPI; blue). Scale bar = 50 μ m (a, c), 20 μ m (b).

of LGR5, Ki67, E-cadherin, Mucin2, and Villin2 in the small intestine of bovine Apo-IOs. These results showed that LGR5, Ki67, Mucin2, F-actin, and E-cadherin were expressed in similar cellular locations as in bovine Bo-IOs³⁷. This indicates that bovine Apo-IOs consisted of various cell types, similar to those of the actual intestinal epithelium. Notably, the expression levels of Mucin2, Villin2, and Ki67 were significantly higher in Bo-IOs than in Apo-IOs, whereas no significant differences were observed in the expression of LGR5 and E-cadherin. In porcine models, LGR5 expression has been demonstrated to be significantly higher in Bo-IOs than in Apo-IOs, with Mucin2 expression showing no significant difference between the two types of organoids³⁸. In addition, the expression of LGR5 and Mucin2 was significantly higher in basal-out than in apical-out organoids, but the expression of Villin2 was lower in dogs. These differences observed between studies are thought to be due to differences among species, culture composition, and culture conditions used. Among the various in vivo cell types, enterocytes have specific receptors and transporters on their apical surface that can absorb amino and fatty acids. To confirm whether Apo-IOs are capable of absorbing nutrients, one of the major functions of the small intestine, fluorescence-labeled fatty (BODIPY) and amino acids were treated with Apo-IOs. The amino acid analogs exhibited blue fluorescence in the nuclear portion of Apo-IOs, whereas BODIPY exhibited green fluorescence in the cytoplasmic portion. Similar to our results, Joo et al.³⁸ and others confirmed that Apo-IOs in pigs absorbed BODIPY cells, whereas Kang and Lee¹⁴ showed that amino acid analogs could be absorbed by chicken Bo-IOs and Apo-IOs. These results suggest that the bovine Apo-IOs constructed in this study possess nutrient uptake functionality.

Human health can be affected by long-term intake of DON-contaminated meat, milk, and eggs^{39–41}. In this study, we performed live/dead assays with DAPI/PI staining to confirm the effect of mycotoxins on small intestinal organoids within a relatively short period (6 h) at DON concentrations of 25 and 50 μM . After DON treatment, the cell viability of bovine Apo-IOs was reduced to approximately 10% within 2 h at a 50 μM DON concentration (data not shown), whereas 25 μM DON reduced cell viability to approximately 48% after 6 h. Based on these results, we treated bovine Apo-IOs with 25 μM DON for 6 h. In a previous chicken study, Apo-IOs were treated with a concentration of approximately 6.75 μM DON for 24 h¹⁴. In contrast, we used a higher concentration of DON over a shorter period to efficiently assess its toxicity in bovine Apo-IOs and to observe the effects of DON. The barrier function, one of the main functions of the small intestine, prevents foreign substances from indiscriminately entering the small intestine. FITC-labeled dextran is commonly used to identify cell barrier functions in vivo and in vitro³⁴. In this study, we confirmed that FITC-4 kDa dextran could not enter organoids, but that it could be introduced into DON-treated Apo-IOs. Although the molecular weight of the dextran used was different, FITC-40 kDa dextran was introduced into chicken Apo-IOs after DON exposure¹⁴. In a study in pigs, when Apo-IOs were treated with FITC-4 kDa dextran, the dextran did not permeate the inside of the Apo-IOs, consistent with our results³⁸. Therefore, our bovine Apo-IOs could be used to identify changes in barrier function caused by mycotoxins, such as DON. The small intestine consists of single-layered epithelial cells that regenerate every 3–5 days, and the crypt-villus structural intestinal stem cells (ISCs) differentiate into various cell types, including enterocytes and goblet, Paneth, and enteroendocrine cells⁴². DON reduces the expression of ISCs, resulting in decreased differentiation and proliferation in the small intestine. For example, goblet cells secrete mucin in the small intestine, which prevents pathogens from attaching to the intestine and protects it from physical and chemical attack⁴³. The reduction in the differentiation and proliferation of goblet cells can be considered a weakening of the barrier function of the small intestine. In this study, we confirmed that the expression of marker genes (LGR5, Ki67, Mucin2, Villin2, and E-cadherin) decreased and that of marker proteins (LGR5, Ki67, Mucin2, E-cadherin, and F-actin) weakened when exposed to DON. DON exposure in small intestine epithelial cells reduces cyclin D expression during the Wnt/ β -catenin signaling process, which induces the decrease of protein levels involved in the system. This reduction is directly linked to the lower expression of LGR5, which inhibits the differentiation of small intestinal epithelial cells⁴⁴. DON also reduces the expression of adherens junction proteins, thereby disrupting epithelial barrier formation in the small intestine⁴⁵. In addition, the weakening of the antioxidant function of mitochondria results in the accumulation of reactive oxygen species, resulting in decreased mucosal formation and impaired barrier function in the small intestine⁴⁶. In this study, the toxic effect of DON was evaluated by the breakdown of Apo-IOs barrier and reducing the expression of small intestine-related genes and proteins. These results also confirm the potential of the Apo-IOs as an in vitro toxicity evaluation model.

The probiotic, *L. plantarum*, is known to attach to and settle in the human intestinal mucosa in the gastrointestinal tract to protect against the host's neutral assistance, immune system protection of mucosal barrier function, xenobiotics, and pathogenic bacteria^{47,48}. In addition, *Lactobacillus* species are known to reduce the toxicity of mycotoxins through hydrophobic bonds, such as those via peptidoglycan, polysaccharides, and teichoic acid in the cell wall⁴⁹. Previous studies have mainly been conducted in pigs^{28,29} and chickens⁵⁰. In this study, approximately 99.8% of the cells were found to be alive during coinoculation of LCS and Apo-IOs, and no significant differences were observed when compared to control. These results show that LCS did not affect the survival rate of Apo-IOs. Although the survival rate of DON + LCS was significantly lower than control group, it showed a noticeable improvement when compared to the survival rate observed with DON alone treatment. These results confirmed that the barrier function was stable during treatment with LCS because FITC-4 kDa dextran did not diffuse into the Apo-IOs as it did in the control group. In the case of DON treatment, the Apo-IOs barrier was broken, and FITC-4 kDa dextran diffused into the organoids. Confirming that *L. plantarum* could alleviate the DON-induced barrier dysfunction, only FITC-4 kDa dextran was found to diffuse across the barrier, unlike during treatment with DON alone. These results suggest that LCS enhanced some barrier functions. Disaccharide activity decreased in the ileum of broiler chickens that were fed DON, and these results showed that the height of the villi decreased after DON exposure, resulting in a decrease in the level of disaccharidase. However, treatment with *L. plantarum* JM113 prevented DON-induced villous damage. In addition, *L. plantarum* JM113 increased the expression of the mucosal defense proteins, polymeric immunoglobulin receptor

and β -defensin-8, thereby reducing DON-induced barrier dysfunction and apoptosis⁵⁰. To determine the effects of LCS on DON, we compared the gene and protein expression between control and LCS. The results confirmed that intestinal function was improved, where significant increases in the gene expression of ISC ability (LGR5), proliferation ability (Ki67), mucosal function (Mucin2), and adherens junction-related factor (E-cadherin) markers were observed. However, there was no significant difference in the gene expression of Villin2. These results show that LCS has a mycotoxin-reducing effect on genes, except for Villin2, in Apo-IOs. For protein expression, LGR5 was partially expressed in the DON-treated group, but strongly expressed in the DON + LCS group. Additionally, Ki67 and F-actin were not expressed in the DON-treated group, but partially expressed in the DON + LCS group. However, Mucin2 was not expressed in the DON-treated group, and E-cadherin was only partially expressed, similar to that observed in the DON-treated group. This result confirmed that when Apo-IOs were treated with LCS, the toxicity of DON was reduced and the expression of some proteins increased. A previous study confirmed that the expression of LGR5 and Ki67 increased when mouse Bo-IOs were treated with *L. reuteri* for eight days⁵¹. Additionally, when various species of *Lactobacillus* were fed to chickens, the number of goblet cells in the small intestine and Mucin2 mRNA expression increased⁵². These results are consistent with those of the present study. However, in the case of Villin2, Du et al.⁵³ confirmed that feeding probiotic *Bacillus* to piglets improved the length of the villi, which grew densely, and increased the expression of villus-related mRNA. DON + LCS resulted in a significantly higher expression of intestinal-related genes than DON alone did. Unlike previous studies, the gene and protein expression observed in this study did not show a reduction effect of mycotoxins on some genes and proteins. This could be due to a variety of factors, such as the concentration and time of treatment of mycotoxins and the concentration of reducing agents used. However, this study confirms the potential application of the Apo-IOs as an in vitro test model for assessing mycotoxin-reducing agent.

Conclusions

In this study, we induced Apo-IOs from Bo-IOs and analyzed their properties and functions. The constructed Apo-IOs were composed of various cells, similar to the actual small intestine, and capable of not only absorbing nutrients but also functioning as an intestinal barrier. In addition, the toxic effects of DON were confirmed through exposing Apo-IOs to it for a relatively short period and by confirming a consequent decrease in barrier function and intestine-related factors. Further, when DON and LCS were co-treated, the toxic effects on barrier function and intestine-related factors in Apo-IOs were reduced. Therefore, Apo-IOs constructed in this study can potentially be applied to evaluate various types of fungal-mediated toxic damage that affect livestock industry productivity and to verify the efficacy of mitigants. Furthermore, these organoids could be used to replace several animal experiments, thereby reducing the number of experimental animals required and enhancing animal welfare. However, in vivo toxic responses to mycotoxins involve complex interactions with both gut microbiota and immune cells. Currently, limitations exist in co-culturing Apo-IOs with gut microbiota and immune cells. Therefore, developing a more advanced in vitro model by improving the culture system to facilitate effective co-culturing with gut microbiota and immune cells is imperative.

Methods

Experimental design

The Bo-IOs was produced by separating the tissue with the crypt from the small intestine tissue, then 3D-cultured in Matrigel and re-cultured to produce the Apo-IOs (Fig. 4a). In this study, the expression of Apo-IOs genes and proteins was investigated, and functional analysis was performed by checking the absorption of amino and fatty acids using fluorescent substances (Fig. 4b). Additionally, we determined the LC50 (Lethal Concentration 50) value of DON using the 4',6-diamidino-2-phenylindole/propidium iodide (DAPI/PI) method. Afterwards, Apo-IOs were treated with DON alone, and a DON + *Lactobacillus plantarum* ATCC14917 culture supernatant

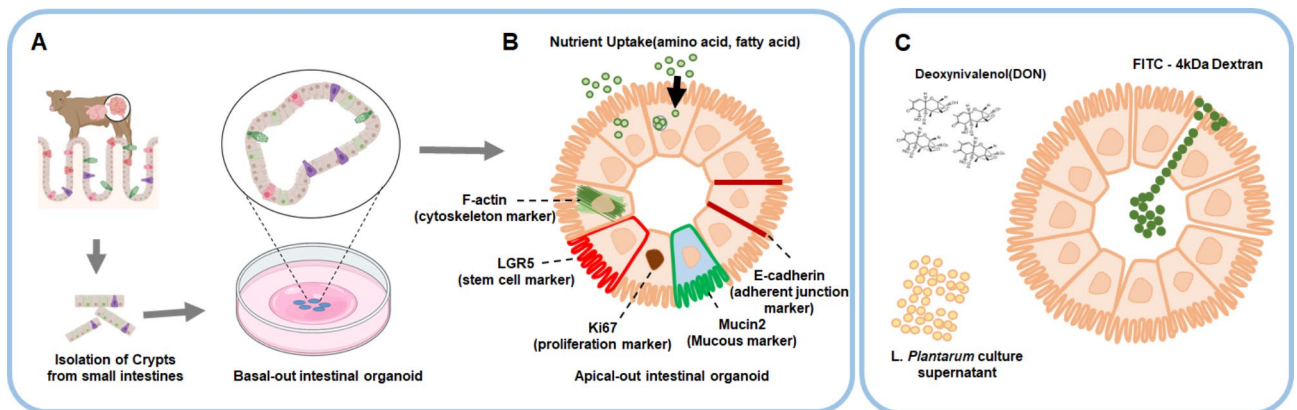


Fig. 4. Experimental design. **a** Establishment of a bovine intestinal organoid with small intestine-derived stem cells. **b** Induction and characterization of a bovine apical-out intestinal organoid. **c** In vitro model for evaluating the toxicity of mycotoxins.

(LCS) combination (DON + LCS). Then, FITC-4 kDa dextran was used to assess intestinal barrier function and the gene and protein expression levels were compared among the different treatments (Fig. 4c).

Establishment and treatment of bovine apical-out intestinal organoids

We isolated crypts from the bovine small intestine and generated organoids using a previously described method³⁷. Briefly, the dome of the organoid was pipetted with 1 mL organoid harvest solution (Bio-technie, Minneapolis, MN, USA) and transferred to a 15 mL tube, whereafter 2 mL cold phosphate buffered saline (PBS) was added for centrifugation. The sample was left stationary at 4 °C for 1 h to remove the Matrigel. After centrifugation at 300 × g for 5 min at 4 °C, intestinal human organoid medium was added to the resulting pellet. To produce organoids in the apical-out form, organoid pieces were cultured at 37 °C for two days by adding 1 mL intestinal human organoid medium to an ultralow-attachment plate⁵⁴. The Apo-IOs were either untreated (control) or exposed to 25 μM DON, LCS, and 25 μM DON + LCS at 37 °C for 6 h to determine the effectiveness of mycotoxins and toxin reducers.

Preparation of bacteria

The *L. plantarum* ATCC14917 strain was cultured to the stationary phase (for approximately 24 h) in sterile Man–Rogosa–Sharpe medium at 37 °C in an anaerobic environment, then centrifuged at 5000 × g for 10 min at 4 °C. After optical density measurements (absorbance at 600 nm = 1.0 ± 0.1 corresponded to 1.0 × 10⁸ CFU/mL), bacteria were harvested via centrifugation at 5000 × g for 10 min at 4 °C. For cell culture assays, the LCS was reserved for subsequent treatment at a 10% (v/v) concentration.

RNA extraction and quantitative real-time PCR

TRIzol reagent (Life Technologies, Carlsbad, CA, USA) was used to extract RNA from the Apo-IOs. The cDNA was synthesized via reverse transcription of RNA using the Superscript IV First-Strand Synthesis System (Invitrogen, Wilmington, DE, USA). The PCR reaction mixture was prepared using a combination of 1 μL cDNA, 1 μL of 10 pmol forward and reverse primers, 7 μL nuclease-free water, and 10 μL power SYBR Green PCR Master Mix (Thermo Fisher Scientific, Waltham, MA, USA) to a final volume of 20 μL. Real-time PCR conditions were set as follows: 95 °C, 30 s; 40 amplification cycles (95 °C, 30 s; 60 °C, 30 s; 95 °C, 30 s); elongation step at 72 °C. Non-specific amplification was confirmed using the melting curve. The Ct value refers to the cycle number at which a fluorescent signal is expressed, and gene expression was quantified using the 2^{-ΔΔCt} method. The qPCR primer used was for 18 S rRNA, and the target genes are shown in Table 1. The qPCR analysis was performed using a Step One Plus real-time PCR system (Applied Biosystems, Waltham, MA, USA).

Immunofluorescence staining of apical-out intestinal bovine organoids

Apo-IOs were washed three times with cold PBS for 5 min and treated with 4% cold paraformaldehyde (Sigma-Aldrich, St. Louis, MO, USA) for 1 h at room temperature. The organoids were washed three times with PBS to remove the fixative and then treated with a permeabilization solution (Thermo Fisher Scientific) at room temperature for 15 min. After washing again with PBS three times, the organoids were treated with a blocking solution (Thermo Fisher Scientific) at room temperature for 1 h. Afterwards, anti-LGR5 (1:200; Cat. No. ab75732; Abcam, Cambridge, UK), anti-Ki67 (1:200; Cat. no. ab1667; Abcam), anti-E-cadherin (1:200; Cat. no. 61081; BD Biosciences, Franklin Lakes, NJ, USA), anti-F-actin (1:200; Cat. no. ab83746; Abcam), and anti-Mucin2 (1:200; Cat. no. Sc-515032; Santa Cruz Biotechnology, Dallas, TX, USA) antibodies were appropriately diluted in the blocking solution. The organoids were treated with these antibodies at 4 °C for 24 h, whereafter they were treated with Alexa Fluor-633 goat anti-mouse IgG (Cat. no. A21052; Thermo Fisher Scientific), Alexa Fluor-488 anti-mouse IgG (Cat. no. A11001; Thermo Fisher Scientific), and Alexa Fluor-488 anti-rabbit IgG (Cat. no. A21441; Thermo Fisher Scientific) antibodies at 4 °C for 24 h. Finally, the Apo-IOs were treated with DAPI (Cat. no. R37606; Thermo Fisher Scientific) for 20 min and then analyzed using a high-resolution confocal laser-scanning microscope (Nikon Instruments Inc., Tokyo, Japan).

Scanning electron microscopy

Apo-IOs were fixed in 2.5% buffered glutaraldehyde in 1× PBS for 2 h at 4 °C, followed by three washes with 0.1 M sodium cacodylate buffer, each wash lasting 10 min. Apo-IOs were post-fixed for 2 h at room temperature in 2% osmium tetroxide in 0.1 M cacodylate buffer, followed by two washes with 0.1 M cacodylate buffer for 10 min each and one wash with distilled water. Apo-IOs were then serially dehydrated in a graded ethanol series (30%, 50%, 70%, 80%, 90%, and two 100% ethanol steps), with each step lasting 10 min. After the ethanol dehydration series, samples were further dehydrated in a 1:1 mixture of ethanol and hexamethyldisilazane (HMDS), followed

Gene name	Forward (5′–3′)	Reverse (5′–3′)
18 S rRNA	GTA ACC CGT TGA ACC CCA TT	CCA TCC AAT CGG TAG TAG CG
LGR5	ACT TTC CAG CAG TTG TTC AGC	GAA TAG ACG ACA GGC GGT TG
Mucin2	TTC GAC GGG AGG AAG TAC AC	TTC ACC GTC TGC TTC ATT CAG
Ki67	AAG ATT CCA GCG CCC ATT CA	TGA GGA ACG AAC ACG ACT GG
Villin	ACC TTC ACA GGC TGG TTC CT	GGT TTT GTT GCT TCC AT
E-cadherin	CCA GGT GAC CAC ACT TGA TG	ATA CAC ATT GTC CCG GGT GT

Table 1. Primers used for the gene expression analysis of intestinal organoids.

by two additional 1-h incubations in 100% HMDS. After infiltration with pure HMDS, Apo-IOs were allowed to dry overnight in a fume hood at room temperature. Following drying, Apo-IOs were mounted onto carbon tape on an SEM stub. Apo-IOs were then coated with a Pt layer using an ion sputter coater (Hitachi E-1045, Hitachi Co.) with the following parameters: 15 mA for 60 s for the front face and 15 mA for 20 s for each lateral side. For SEM imaging, Apo-IOs were examined using the SE mode (ETD detector) on a TeneoVS SEM (FEI, USA). Images were captured at a resolution of 3072 pixels \times 2048 pixels, with a working distance of approximately 10.0 mm, an acceleration voltage of 5 kV, and an emission current of 50 pA.

Fatty acid absorption of apical-out intestinal bovine organoids

After washing the Apo-IOs with cold PBS three times, BODIPY 500/510 C1, C12 (Invitrogen) and fatty acid-free BSA were combined to a final concentration of 5 μ M/L, which was then added to the organoids. The organoids were then incubated at 37 °C in a CO₂ incubator for 30 min. Fluorescent samples were seeded and mounted onto glass slides. Representative images were obtained using a confocal laser-scanning microscope (Nikon Instruments Inc., Tokyo, Japan).

Amino acid absorption of apical-out intestinal bovine organoids

The Apo-IOs were transferred to 15-mL conical tubes and centrifuged at 300 \times g for 5 min. The supernatant was removed and the cells washed three times with prewarmed HBSS (Cat. no. 14175095; Thermo Fisher Scientific). A prewarmed BPA uptake solution (Cat. no. UP02; Dojindo, Kumamoto, Japan) was added to the Apo-IOs, which were then incubated at 37 °C for 5 min and centrifuged thereafter for 5 min at 300 \times g. The supernatant was removed, and a prewarmed working solution (Cat. no. UP02; Dojindo) added to the organoids that were then incubated at 37 °C in a CO₂ incubator for 5 min. Fluorescent samples were seeded and mounted onto glass slides. Representative images were obtained using a confocal laser-scanning microscope.

Epithelial barrier permeability of apical-out bovine organoids

Untreated Apo-IOs, as well as those treated with 25 μ M DON, LCS, and 25 μ M DON + LCS for 6 h, were exposed to FITC-4 kDa dextran (50 ng/mL; Sigma-Aldrich), and the penetration of FITC-4 kDa dextran into the Apo-IOs then confirmed using a confocal laser-scanning microscope.

Cell viability assay

The DAPI/PI assay was used to assess the cell viability of Apo-IOs in response to DON and LCS exposure. Untreated Apo-IOs, as well as those treated with 25 μ M DON, LCS, and 25 μ M DON + LCS for 6 h, were exposed to PI. After washing three times with cold PBS, 4% formaldehyde and DAPI were added for 15 min. Cell viability was then assessed using a confocal laser-scanning microscope.

Statistical analysis

Statistical analyses were performed using GraphPad Prism (version 9; GraphPad Software, La Jolla, CA, USA). Statistical significance was determined using a t-test or one-way ANOVA, with corrections for multiple comparisons, as appropriate. Data are presented as the mean \pm SD, and P-values < 0.05, < 0.01, < 0.001, and < 0.0001 were considered statistically significant. All experiments were performed at least three times.

Data availability

The data that support the findings of this study are available from the corresponding author upon reasonable request.

Received: 12 July 2024; Accepted: 10 December 2024

Published online: 28 December 2024

References

- Lancaster, M. A. & Knoblich, J. A. Organogenesis in a dish: Modeling development and disease using organoid technologies. *Science* **345**, 1247125. <https://doi.org/10.1126/science.1247125> (2014).
- Tuveson, D. & Clevers, H. Cancer modeling meets human organoid technology. *Science* **364**, 952–955. <https://doi.org/10.1126/science.aaw6985> (2019).
- Sato, T. et al. Single Lgr5 stem cells build crypt-villus structures in vitro without a mesenchymal niche. *Nature* **459**, 262–265. <https://doi.org/10.1038/nature07935> (2009).
- Fujii, M. et al. Human intestinal organoids maintain self-renewal capacity and cellular diversity in niche-inspired culture condition. *Cell Stem Cell* **23**, 787–793. <https://doi.org/10.1016/j.stem.2018.11.016> (2018). e786.
- Powell, R. H. & Behnke, M. S. WRN conditioned media is sufficient for in vitro propagation of intestinal organoids from large farm and small companion animals. *Biol. Open* **6**, 698–705. <https://doi.org/10.1242/bio.021717> (2017).
- Pierzchalska, M. et al. Probiotic Lactobacillus acidophilus bacteria or synthetic TLR2 agonist boost the growth of chicken embryo intestinal organoids in cultures comprising epithelial cells and myofibroblasts. *Comp. Immunol. Microbiol. Infect. Dis.* **53**, 7–18. <https://doi.org/10.1016/j.cimid.2017.06.002> (2017).
- Li, L. et al. Porcine intestinal enteroids: A new model for studying enteric coronavirus porcine epidemic diarrhea virus infection and the host innate response. *J. Virol.* **93** <https://doi.org/10.1128/jvi.01682-18> (2019).
- Yin, L. et al. Not interferon responses, determines the intestinal segmental tropism of porcine deltacoronavirus. *J. Virol.* **94** <https://doi.org/10.1128/jvi.00480-20> (2020). Aminopeptidase N Expression.
- Li, Y. et al. Next-generation porcine intestinal organoids: an apical-out organoid model for swine enteric virus infection and immune response investigations. *J. Virol.* **94** <https://doi.org/10.1128/jvi.01006-20> (2020).
- Luo, H. et al. Utility evaluation of porcine enteroids as PDCoV infection model in vitro. *Front. Microbiol.* **11**, 821. <https://doi.org/10.3389/fmicb.2020.00821> (2020).
- Li, X. G. et al. Acute exposure to deoxynivalenol inhibits porcine enteroid activity via suppression of the Wnt/ β -catenin pathway. *Toxicol. Lett.* **305**, 19–31. <https://doi.org/10.1016/j.toxlet.2019.01.008> (2019).

12. Chelakkot, C., Ghim, J. & Ryu, S. H. Mechanisms regulating intestinal barrier integrity and its pathological implications. *Exp. Mol. Med.* **50**, 1–9. <https://doi.org/10.1038/s12276-018-0126-x> (2018).
13. Belair, D. G. et al. Human ileal organoid model recapitulates clinical incidence of diarrhea associated with small molecule drugs. *Toxicol. Vitro*. **68**, 104928. <https://doi.org/10.1016/j.tiv.2020.104928> (2020).
14. Kang, T. H. & Lee, S. I. Establishment of a chicken intestinal organoid culture system to assess deoxynivalenol-induced damage of the intestinal barrier function. *J. Anim. Sci. Biotechnol.* **15**, 30. <https://doi.org/10.1186/s40104-023-00976-4> (2024).
15. Marin, S., Ramos, A. J., Cano-Sancho, G. & Sanchis, V. Mycotoxins: Occurrence, toxicology, and exposure assessment. *Food Chem. Toxicol.* **60**, 218–237. <https://doi.org/10.1016/j.fct.2013.07.047> (2013).
16. Pestka, J. J. Deoxynivalenol: Toxicology and potential effects on humans. *J. Toxicol. Environ. Health B Crit. Rev.* **8**, 39–69. <https://doi.org/10.1080/10807030500000000> (2005).
17. Ghareeb, K., Awad, W. A., Böhm, J. & Zebeli, Q. Impacts of the feed contaminant deoxynivalenol on the intestine of monogastric animals: Poultry and swine. *J. Appl. Toxicol.* **35**, 327–337. <https://doi.org/10.1002/jat.3083> (2015).
18. Pestka, J. J. Deoxynivalenol: Mechanisms of action, human exposure, and toxicological relevance. *Arch. Toxicol.* **84**, 663–679. <https://doi.org/10.1007/s00204-010-0579-8> (2010).
19. Pinton, P. et al. Deoxynivalenol impairs porcine intestinal barrier function and decreases the protein expression of claudin-4 through a mitogen-activated protein kinase-dependent mechanism. *J. Nutr.* **140**, 1956–1962. <https://doi.org/10.3945/jn.110.123919> (2010).
20. Payros, D. et al. The food contaminant, deoxynivalenol, modulates the Thelper/Treg balance and increases inflammatory bowel diseases. *Arch. Toxicol.* **94**, 3173–3184. <https://doi.org/10.1007/s00204-020-02817-z> (2020).
21. Bocsik, A. et al. Reversible opening of intercellular junctions of intestinal epithelial and brain endothelial cells with tight junction modulator peptides. *J. Pharm. Sci.* **105**, 754–765. <https://doi.org/10.1016/j.xphs.2015.11.018> (2016).
22. De Walle, J. V. et al. Deoxynivalenol affects in vitro intestinal epithelial cell barrier integrity through inhibition of protein synthesis. *Toxicol. Appl. Pharmacol.* **245**, 291–298. <https://doi.org/10.1016/j.taap.2010.03.012> (2010).
23. Lessard, M. et al. Impact of deoxynivalenol (DON) contaminated feed on intestinal integrity and immune response in swine. *Food Chem. Toxicol.* **80**, 7–16. <https://doi.org/10.1016/j.fct.2015.02.013> (2015).
24. Gao, Y., Meng, L., Liu, H. & Wang, J. & Zheng, N. The compromised intestinal barrier induced by mycotoxins. *Toxins* **12** (2020).
25. Maidana, L., de Souza, M. & Bracarense, A. Lactobacillus plantarum and deoxynivalenol detoxification: A concise review. *J. Food Prot.* **85**, 1815–1823. <https://doi.org/10.4315/jfp-22-077> (2022).
26. Dallagnol, A. M., Bustos, A. Y., Martos, G. I., Valdez, G. F. & Gerez, C. L. Antifungal and antimycotoxigenic effect of Lactobacillus plantarum CRL 778 at different water activity values. *Rev. Argent. Microbiol.* **51**, 164–169. <https://doi.org/10.1016/j.ram.2018.04.004> (2019).
27. Eun, C. S. et al. Lactobacillus casei prevents impaired barrier function in intestinal epithelial cells. *APMIS* **119**, 49–56. <https://doi.org/10.1111/j.1600-0463.2010.02691.x> (2011).
28. Maidana, L. G., Gerez, J., Hohmann, M. N. S., Verri, W. A. Jr. & Bracarense, A. Lactobacillus plantarum metabolites reduce deoxynivalenol toxicity on jejunal explants of piglets. *Toxicon* **203**, 12–21. <https://doi.org/10.1016/j.toxicon.2021.09.023> (2021).
29. Maidana, L. G., Gerez, J., Pinho, F., Garcia, S. & Bracarense, A. Lactobacillus plantarum culture supernatants improve intestinal tissue exposed to deoxynivalenol. *Exp. Toxicol. Pathol.* **69**, 666–671. <https://doi.org/10.1016/j.etp.2017.06.005> (2017).
30. Park, K. W. et al. Effect of wnt signaling pathway activation on the efficient generation of bovine intestinal organoids. *J. Anim. Reprod. Biotechnol.* **37**, 136–143. <https://doi.org/10.12750/JARB.37.2.136> (2022).
31. Bartfeld, S. et al. In vitro expansion of human gastric epithelial stem cells and their responses to bacterial infection. *Gastroenterology* **148**, 126–136.e126. <https://doi.org/10.1053/j.gastro.2014.09.042> (2015).
32. Bartfeld, S. & Clevers, H. Organoids as Model for Infectious diseases: Culture of human and murine stomach organoids and microinjection of Helicobacter Pylori. *J. Vis. Exp.* <https://doi.org/10.3791/53359> (2015).
33. VanDussen, K. L. et al. Development of an enhanced human gastrointestinal epithelial culture system to facilitate patient-based assays. *Gut* **64**, 911–920. <https://doi.org/10.1136/gutjnl-2013-306651> (2015).
34. Co, J. Y., Margalef-Català, M., Monack, D. M. & Amieva, M. R. Controlling the polarity of human gastrointestinal organoids to investigate epithelial biology and infectious diseases. *Nat. Protoc.* **16**, 5171–5192. <https://doi.org/10.1038/s41596-021-00607-0> (2021).
35. Kakni, P. et al. Hypoxia-tolerant apical-out intestinal organoids to model host-microbiome interactions. *J. Tissue Eng.* **14**, 20417314221149208. <https://doi.org/10.1177/20417314221149208> (2023).
36. Sato, T. et al. Long-term expansion of epithelial organoids from human colon, adenoma, adenocarcinoma, and Barrett's epithelium. *Gastroenterology* **141**, 1762–1772. <https://doi.org/10.1053/j.gastro.2011.07.050> (2011).
37. Lee, B. R. et al. Robust three-dimensional (3D) expansion of bovine intestinal organoids: An in vitro model as a potential alternative to an in vivo system. *Animals* **11** (2021).
38. Joo, S. S. et al. Porcine intestinal apical-out organoid model for gut function study. *Anim. (Basel)*. **12**. <https://doi.org/10.3390/ani12030372> (2022).
39. Mishra, S., Srivastava, S., Dewangan, J., Divakar, A. & Kumar Rath, S. Global occurrence of deoxynivalenol in food commodities and exposure risk assessment in humans in the last decade: A survey. *Crit. Rev. Food Sci. Nutr.* **60**, 1346–1374. <https://doi.org/10.1080/10408398.2019.1571479> (2022).
40. Mousavi Khaneghah, A., Farhadi, A., Nematollahi, A., Vasseghian, Y. & Fakhri, Y. A systematic review and meta-analysis to investigate the concentration and prevalence of trichothecenes in the cereal-based food. *Trends Food Sci. Technol.* **102**, 193–202. <https://doi.org/10.1016/j.tifs.2020.05.026> (2020).
41. Wang, L. et al. Food raw materials and food production occurrences of deoxynivalenol in different regions. *Trends Food Sci. Technol.* **83**, 41–52. <https://doi.org/10.1016/j.tifs.2018.11.003> (2019).
42. Rizk, P. & Barker, N. Gut stem cells in tissue renewal and disease: Methods, markers, and myths. *Wiley Interdiscip. Rev. Syst. Biol. Med.* **4**, 475–496. <https://doi.org/10.1002/wsbm.1176> (2012).
43. Schwerdtfeger, L. A. & Tobet, S. A. Vasoactive intestinal peptide regulates ileal goblet cell production in mice. *Physiol. Rep.* **8**, e14363. <https://doi.org/10.14814/phy2.14363> (2020).
44. Hanyu, H. et al. Mycotoxin Deoxynivalenol has different impacts on intestinal barrier and stem cells by its Route of exposure. *Toxins (Basel)*. **12**. <https://doi.org/10.3390/toxins12100610> (2020).
45. Pinton, P. et al. Toxicity of deoxynivalenol and its acetylated derivatives on the intestine: Differential effects on morphology, barrier function, tight junction proteins, and mitogen-activated protein kinases. *Toxicol. Sci.* **130**, 180–190. <https://doi.org/10.1093/toxsci/kfs239> (2012).
46. Banan, A., Choudhary, S., Zhang, Y., Fields, J. Z. & Keshavarzian, A. Oxidant-induced intestinal barrier disruption and its prevention by growth factors in a human colonic cell line: Role of the microtubule cytoskeleton. *Free Radic. Biol. Med.* **28**, 727–738. [https://doi.org/10.1016/s0891-5849\(00\)00160-x](https://doi.org/10.1016/s0891-5849(00)00160-x) (2000).
47. Lightfoot, Y. L. et al. SIGNR3-dependent immune regulation by Lactobacillus acidophilus surface layer protein A in colitis. *Embo j.* **34**, 881–895. <https://doi.org/10.15252/embj.201490296> (2015).
48. Rao, R. K. & Samak, G. Protection and restitution of gut barrier by probiotics: Nutritional and clinical implications. *Curr. Nutr. Food Sci.* **9**, 99–107. <https://doi.org/10.2174/1573401311309020004> (2013).

49. Chlebicz, A. & Ślizewska, K. Vitro detoxification of aflatoxin B(1), Deoxynivalenol, Fumonisin, T-2 toxin and Zearalenone by probiotic Bacteria from Genus Lactobacillus and Saccharomyces cerevisiae yeast. *Probiotics Antimicrob. Proteins*. **12**, 289–301. <https://doi.org/10.1007/s12602-018-9512-x> (2020).
50. Yang, X. et al. Gut microbiota mediates the protective role of Lactobacillus plantarum in ameliorating deoxynivalenol-induced apoptosis and intestinal inflammation of broiler chickens. *Poult. Sci.* **99**, 2395–2406. <https://doi.org/10.1016/j.psj.2019.10.034> (2020).
51. Wu, H. et al. Lactobacillus reuteri maintains intestinal epithelial regeneration and repairs damaged intestinal mucosa. *Gut Microbes*. **11**, 997–1014. <https://doi.org/10.1080/19490976.2020.1734423> (2020).
52. Cao, L., Yang, X., Sun, F., Liu, C. & Yao, J. Lactobacillus strain with high adhesion stimulates intestinal mucin expression in Broiler. *J. Poult. Sci.* **49**, 273–281. <https://doi.org/10.2141/jpsa.0110146> (2012).
53. Du, W. et al. Probiotic Bacillus enhance the intestinal epithelial cell barrier and immune function of piglets. *Benef Microbes*. **9**, 743–754. <https://doi.org/10.3920/bm2017.0142> (2018).
54. Co, J. Y. et al. Controlling epithelial polarity: A human enteroid model for host-Pathogen interactions. *Cell. Rep.* **26**, 2509–2520e2504. <https://doi.org/10.1016/j.celrep.2019.01.108> (2019).

Acknowledgements

Not applicable.

Author contributions

Conceptualization: JGY and MGL. Experimental conduction: MGL, BRL, SYC, JHK, PYL, and MHO. Laboratory analysis: MGL and BRL. Experimental supervision: JGY. Data analysis and interpretation: JGY and MGL. Original draft writing: MGL. Draft revision: BRL, SYC, JHK, PYL, MHO, and JGY.

Funding

This work was carried out with the support of “Cooperative Research Program for Agriculture Science and Technology Development (Project No. PJ01671901)” Rural Development Administration(RDA), Republic of Korea.

Declarations

Competing interests

The authors declare no competing interests.

Ethics approval and consent to participate

Experimental use of bovine-derived material was approved by the Institutional Animal Care and Use Committee (IACUC) of the National Institute of Animal Science (NIAS-2019-366), Korea. All methods of this study were carried out in accordance with relevant guidelines and regulations. The study was confirmed and followed in accordance with ARRIVE guidelines. All authors were personally and actively involved in the substantial work leading to this paper, taking public responsibility for its content.

Additional information

Correspondence and requests for materials should be addressed to J.G.Y.

Reprints and permissions information is available at www.nature.com/reprints.

Publisher's note Springer Nature remains neutral with regard to jurisdictional claims in published maps and institutional affiliations.

Open Access This article is licensed under a Creative Commons Attribution-NonCommercial-NoDerivatives 4.0 International License, which permits any non-commercial use, sharing, distribution and reproduction in any medium or format, as long as you give appropriate credit to the original author(s) and the source, provide a link to the Creative Commons licence, and indicate if you modified the licensed material. You do not have permission under this licence to share adapted material derived from this article or parts of it. The images or other third party material in this article are included in the article's Creative Commons licence, unless indicated otherwise in a credit line to the material. If material is not included in the article's Creative Commons licence and your intended use is not permitted by statutory regulation or exceeds the permitted use, you will need to obtain permission directly from the copyright holder. To view a copy of this licence, visit <http://creativecommons.org/licenses/by-nc-nd/4.0/>.

© The Author(s) 2024